Noname manuscript No.
(will be inserted by the editor)

Mechanisms of the 2014-2016 Delayed Super El Niño Captured by Simple Dynamical Models (Supplementary Material)

Sulian Thual · Andrew J. Majda · Nan Chen

Received: date / Accepted: date

The present supplementary material is organized as follows. Section 1 details the formulation of the ENSO model used in the present article. Section 2 provides additional examples of delayed, super and moderate El Niño events in the model. Section 3 provides additional details on the ensemble runs including the evolution of ensemble mean and standard deviation. Section 4 repeats results from the main body of the article in the more complete model version from (Chen and Majda, 2016, 2017) to show the similarity of results.

1 ENSO Model

We present here the ENSO model used in the article. Such a model is identical to the one of Thual et al (2016) and succeeds in recovering the traditional El Niño and occasional super El Niño in the eastern Pacific with realistic buildup and shutdown of wind bursts. The model is recalled here for completeness, including the parametrization of stochastic wind bursts shown in the main

Sulian Thual
Department of Mathematics, and Center for Atmosphere Ocean Science, Courant Institute of Mathematical Sciences, New York University, 251 Mercer Street, New York, NY 10012 USA
E-mail: sulian.thual@gmail.com

Andrew J. Majda
Department of Mathematics, and Center for Atmosphere Ocean Science, Courant Institute of Mathematical Sciences, New York University, 251 Mercer Street, New York, NY 10012 USA, and Center for Prototype Climate Modeling, New York University Abu Dhabi, Saadiyat Island, Abu Dhabi, UAE.
E-mail: jonjon@cims.nyu.edu

Nan Chen
Department of Mathematics, and Center for Atmosphere Ocean Science, Courant Institute of Mathematical Sciences, New York University, 251 Mercer Street, New York, NY 10012 USA
E-mail: chennan@cims.nyu.edu (corresponding author)

article. Note that a more complete model version (Chen and Majda, 2016, 2017) includes nonlinear advection of SST that facilitates the occurrence of the central Pacific El Niño, as shown hereafter at the end of the supplementary information. For even more details on the model see Thual et al (2016) that provides in particular all informations on parameters values and numerical solving.

1.1 Coupled ENSO model

The starting ENSO model from Thual et al (2016) consists of a non-dissipative atmosphere coupled to a simple shallow-water ocean and SST budget:

Interannual atmosphere model

$$\begin{aligned} &-yv - \partial_x\theta = 0 \\ &yu - \partial_y\theta = 0 \\ &-(\partial_x u + \partial_y v) = E_q/(1-\overline{Q}), \end{aligned} \tag{1}$$

Interannual ocean model

$$\begin{aligned} &\partial_\tau U - c_1 YV + c_1\partial_x H = c_1\tau_x \\ &YU + \partial_Y H = 0 \\ &\partial_\tau H + c_1(\partial_x U + \partial_Y V) = 0, \end{aligned} \tag{2}$$

Interannual SST model

$$\partial_\tau T = -c_1\zeta E_q + c_1\eta H \tag{3}$$

with

$$\begin{aligned} E_q &= \alpha_q T \\ \tau_x &= \gamma(u+u_p). \end{aligned} \tag{4}$$

In the above model, x is zonal direction, y and Y are meridional direction in the atmosphere and ocean, respectively, and τ is interannual time. For the atmosphere, u, v are zonal and meridional winds, θ is potential temperature, and E_q is latent heating. For the ocean, U, V, are zonal and meridional currents, H is thermocline depth, τ_x is zonal wind stress and T is SST. All those variables are anomalies from an equilibrium state, and are nondimensional. The u_p is a stochastic wind burst perturbation described hereafter. Note that without this perturbation the above coupled system is linear, deterministic and stable. The atmosphere extends over the entire equatorial belt $0 \le x \le L_A$ with periodic boundary conditions $u(0, y, t) = u(L_A, y, t)$, etc, while the Pacific ocean extends from $0 \le x \le L_O$ with reflection boundary conditions $\int_{-\infty}^{+\infty} U(0, y, t)dy = 0$ and $U(L_O, y, t) = 0$. The $\overline{Q}$, c_1, ζ, α_q and γ are constant parameters of the system while the thermocline feedback parameter $\eta(x)$ is maximal in the eastern Pacific as show in Fig. S1(a). In addition, the meridional axis y and Y are different in the atmosphere and ocean as they each scale to a suitable Rossby radius (see hereafter).

1.2 Stochastic Wind Bursts

The wind bursts activity is driven here by a simple stochastic process that accounts for its irregular, intermittent and unpredictable nature on the interannual timescale as well as its dependence on the western Pacific warm pool strength. The wind bursts perturbations in Eq. 4 read:

$$u_p = a_p(\tau)s_p(x, y), \tag{5}$$

with fixed spatial structure s_p centered in the western Pacific as shown in Fig. S1(b), and amplitude a_p (positive for a WWB and negative for an EWB) that evolves as follows:

$$\frac{da_p}{d\tau} = -d_p a_p + \sigma_p \dot{W}(\tau), \tag{6}$$

where d_p is dissipation and $\dot{W}$ is a white noise source of intensity σ_p.

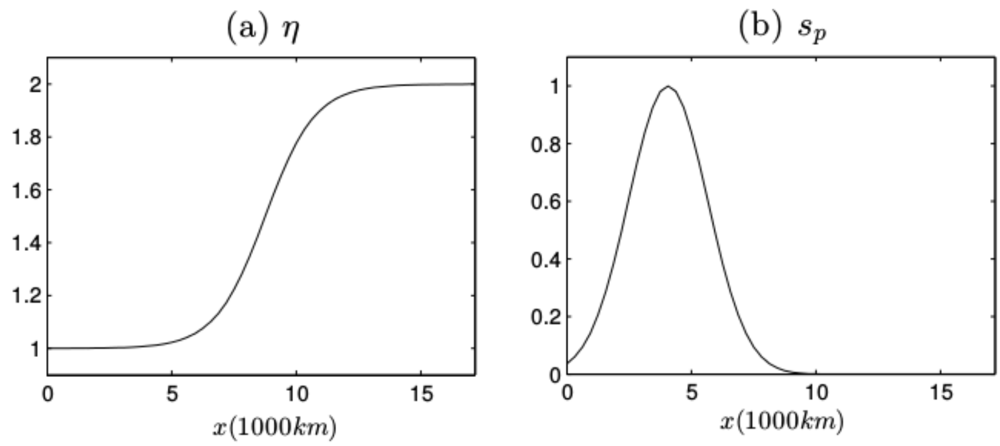

Fig. S1 Model parametrization. (a) thermocline feedback η and (b) wind burst zonal structure s_p at equator, as a function of zonal position x (1000 km).

1.3 Two-states Markov Jump Process

The noise source intensity σ_p described above depends here on the western Pacific warm pool strength. For this, we allow the equatorial Pacific system to switch back and forth between two Markov states with different wind burst characteristics (Lawler, 2006; Majda and Harlim, 2012):

$$\text{if } \sigma_p = \begin{cases} \sigma_{p0} \text{ for the quiescent state 0} \\ \sigma_{p1} \text{ for the active state 1,} \end{cases} \tag{7}$$

whith increased wind burst activity $\sigma_{p1} > \sigma_{p0}$ the in the active state 1. The probabilities of transiting from one state at time τ to the other at time $\tau + \Delta\tau$ read:

$$\begin{aligned}
&P(\sigma_p(\tau+\Delta\tau)=\sigma_{p1}|\sigma_p(\tau)=\sigma_{p0}) = \mu_{01}\Delta\tau + o(\Delta\tau)\\
&P(\sigma_p(\tau+\Delta\tau)=\sigma_{p0}|\sigma_p(\tau)=\sigma_{p1}) = \mu_{10}\Delta\tau + o(\Delta\tau)\\
&P(\sigma_p(\tau+\Delta\tau)=\sigma_{p0}|\sigma_p(\tau)=\sigma_{p0}) = 1-\mu_{01}\Delta\tau + o(\Delta\tau)\\
&P(\sigma_p(\tau+\Delta\tau)=\sigma_{p1}|\sigma_p(\tau)=\sigma_{p1}) = 1-\mu_{10}\Delta\tau + o(\Delta\tau),
\end{aligned} \tag{8}$$

with transition rates μ_{01} and μ_{10} that depend on T_W the average of SST anomalies in the western half of the equatorial Pacific. The transition rates read:

$$\begin{aligned}
\mu_{01} &= (1+\tanh(2T_W))/8\\
\mu_{10} &= (1-\tanh(2T_W))/4
\end{aligned} \tag{9}$$

where a stronger warm pool ($T_W \geq 0$) favors the transition to the active state with increased wind burst activity, and conversely a weaker warm pool ($T_W \leq 0$) favors the transition to the quiescent state. Note that the system can switch more easily from the active state to the quiescent state as shown by the increased amplitude of μ_{10}.

1.4 Meridional Truncation

In order to compute the solutions of the ENSO model, we consider a meridional truncation to the first parabolic cylinder functions different in the ocean and atmosphere as shown in Fig. S2. The first atmospheric parabolic cylinder functions read $\phi_0(y) = (\pi)^{-1/4}exp(-y^2/2)$, $\phi_2 = (4\pi)^{-1/4}(2y^2-1)exp(-y^2/2)$, while the ocean parabolic cylinder functions read $\psi_m(Y)$ where $Y = y/\sqrt{c}$.

In the atmosphere we assume a truncation of latent heating to the first parabolic cylinder function ϕ_0, $E_q = E_q\phi_0(y)$ (with a slight abuse of notations). This is known to excite only the Kelvin and first Rossby atmospheric equatorial waves, of amplitude K_A and R_A. In the ocean, we assume a truncation of zonal wind stress forcing to ψ_0, $\tau_x = \tau_x\psi_0$. This is known to excite only the the Kelvin and first Rossby atmospheric oceanic waves, of amplitude K_O and R_O. Similarly, for the SST model we assume a truncation ψ_0,$T = T\psi_0$. In order to couple the ocean and atmosphere, we introduce projection coefficients that reads $\chi_A = \int_{-\infty}^{+\infty}\phi_0(y)\phi_0(y/\sqrt{c})dy$ and $\chi_O = \int_{-\infty}^{+\infty}\psi_0(Y)\psi_0(\sqrt{c}Y)dY$. We introduce in addition reflection coefficients r_E and r_W for the oceanic Kelvin and Rossby waves consistent with the boundary conditions. The ENSO model truncated meridionally reads:

Interannual atmosphere model

$$\begin{aligned}
&\partial_x K_A = -\chi_A E_q(2-2\overline{Q})^{-1}\\
&-\partial_x R_A/3 = -\chi_A E_q(3-3\overline{Q})^{-1}\\
&K_A(0,\tau) = K_A(L_A,\tau)\\
&R_A(0,\tau) = R_A(L_A,\tau),
\end{aligned} \tag{10}$$

Interannual ocean model

$$
\begin{aligned}
&\partial_\tau K_O + c_1 \partial_x K_O = \chi_O c_1 \tau_x / 2 \\
&\partial_\tau R_O - (c_1/3)\partial_x R_O = -\chi_O c_1 \tau_x / 3 \\
&K_O(0,t) = r_W R_O(0,t) \\
&R_O(L_O,t) = r_E K_O(L_O,t),
\end{aligned}
\tag{11}
$$

Interannual SST model

$$
\partial_\tau T / c_1 = -\zeta E_q + \eta(K_O + R_O),
\tag{12}
$$

Couplings

$$
\begin{aligned}
&E_q = \alpha_q T \\
&\tau_x = \gamma(K_A - R_A).
\end{aligned}
\tag{13}
$$

The reconstructed variables reads:

$$
\begin{aligned}
&u = (K_A - R_A)\phi_0 + (R_A/\sqrt{2})\phi_2 \\
&\theta = -(K_A + R_A)\phi_0 - (R_A/\sqrt{2})\phi_2 \\
&U = (K_O - R_O)\psi_0 + (R_O/\sqrt{2})\psi_2 \\
&H = (K_O + R_O)\psi_0 + (R_O/\sqrt{2})\psi_2.
\end{aligned}
\tag{14}
$$

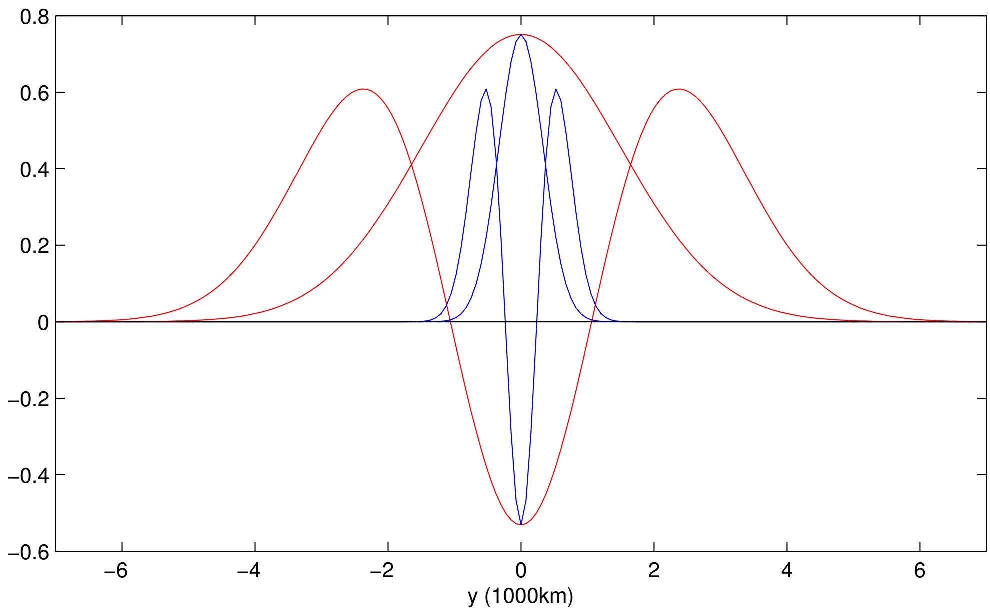

Fig. S2 Meridional profiles of atmosphere parabolic cylinder functions ϕ_0, ϕ_2(red) and ocean parabolic cylinder functions ψ_0, ψ_2(blue), as a function of meridional position y (1000km).

2 Additional Examples of Delayed Super El Niño events

We show here additional examples of El Niño events in the model, as taken from the outputs of the numerical experiment shown in Fig. 2 of the main article. This includes examples of delayed super El Niño events, (Fig. S3), super events (Fig. S4) and moderate events (Fig. S5). In particular, those events vary in strength, structure and intensity depending on the characteristics of wind bursts during their development. All events start with overall favorable conditions of increased SST and thermocline depth in the western Pacific in the active state 1 of wind burst activity. Delayed super El Niño events (Fig. S3) are characterized by both easterly and westerly wind bursts stalling their development before an eventual sequence of strong westerly wind bursts leading to a peaking of SST anomalies. In contrast, super El Niño events (Fig. S4) immediately develop following a strong sequence of westerly wind bursts. Meanwhile, moderate El Niño events (Fig. S5) are characterized by sequences of westerly wind bursts (as well as early easterly wind bursts in some case) that are overall of weaker intensity or duration as compared to super events. Finally, for all those events wind burst activity shutdowns around the event peak (due to the cool SSTs in the western Pacific that switch the system back to the quiescent state of wind burst activity) which initiates a relaxation of conditions towards La Niña.

3 Ensemble Runs

We show here additional details on the ensemble run experiments shown in Fig. 5 and 6 of the main article. All ensemble members (5000 in total) are initiated from initial conditions taken at 204.3 yr in Fig. 2 of the main article, consisting of a recharged state with increased SST and thermocline depth in the western Pacific in the active state of wind burst activity, a situation similar to the one of early 2014 in nature. Fig. S6 shows the evolution of ensemble mean and ensemble standard deviation for those experiments.

The ensemble mean shows an average SST peaking time of events around year 205.5 i.e. one year after the initial recharged conditions. Meanwhile the ensemble standard deviation shows a spread of similar amplitude that develops shortly after the initial conditions. This spread is due to differences in the timing and amplitude of El Niño peaks for each ensemble member, as well as their eventual return to the quiescent state of wind burst activity. Note also that the ensemble mean wind burst amplitude a_p is zero by construction.

4 The Delayed 2014-2016 super El Niño in the complete ENSO model

A more complete version (Chen and Majda, 2016, 2017) of the present ENSO model includes nonlinear advection of SST that facilitates the occurrence of the

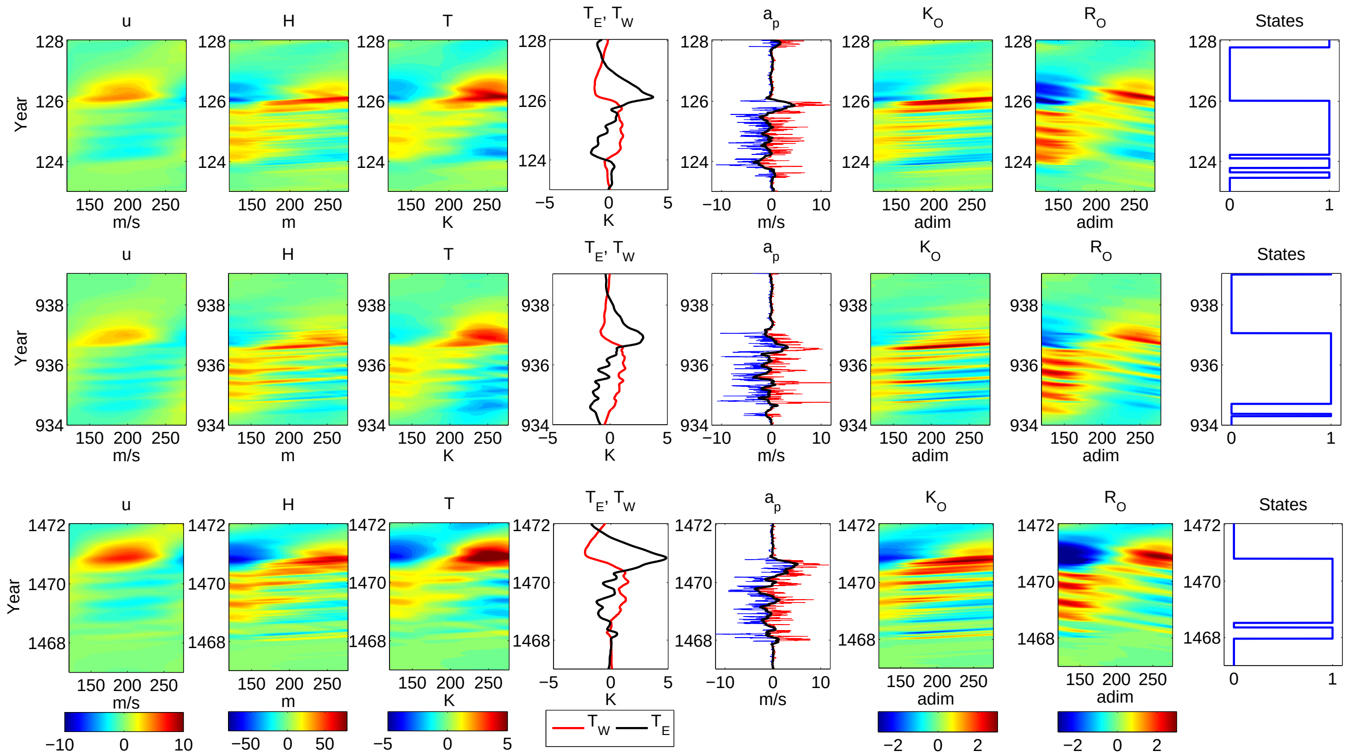

Fig. S3 Additional examples of Delayed super El Niño events in the model, as in Fig. 2 of the main article.

central Pacific El Niño, allowing for more realism including realistic variance and non-Gaussian statistical features in different Niño regions spanning from the western to the eastern Pacific. For simplicity and as we emphasized the role of wind bursts during the 2014-2016 period in the observational record this more complete version has been omitted in the main article in favor of the simpler model version from Thual et al (2016). We repeat here results from the main article with this more complete model version to show that results are qualitatively similar.

We first briefly detail the model modifications in the model from (Chen and Majda, 2016, 2017) as compared to the ENSO model from Thual et al (2016) recalled above. First, the evolution of wind burst amplitude a_p is modified as:

$$\frac{da_p}{d\tau} = -d_p(a_p - \hat{a}_p) + \sigma_p \dot{W}(\tau), \tag{15}$$

where $\hat{a}_p < 0$ accounts for the occasional intensification of the Walker circulation on decadal timescale. Second, we now allow the equatorial Pacific system to switch back and forth between three states $s = 0, 1, 2$ with different wind

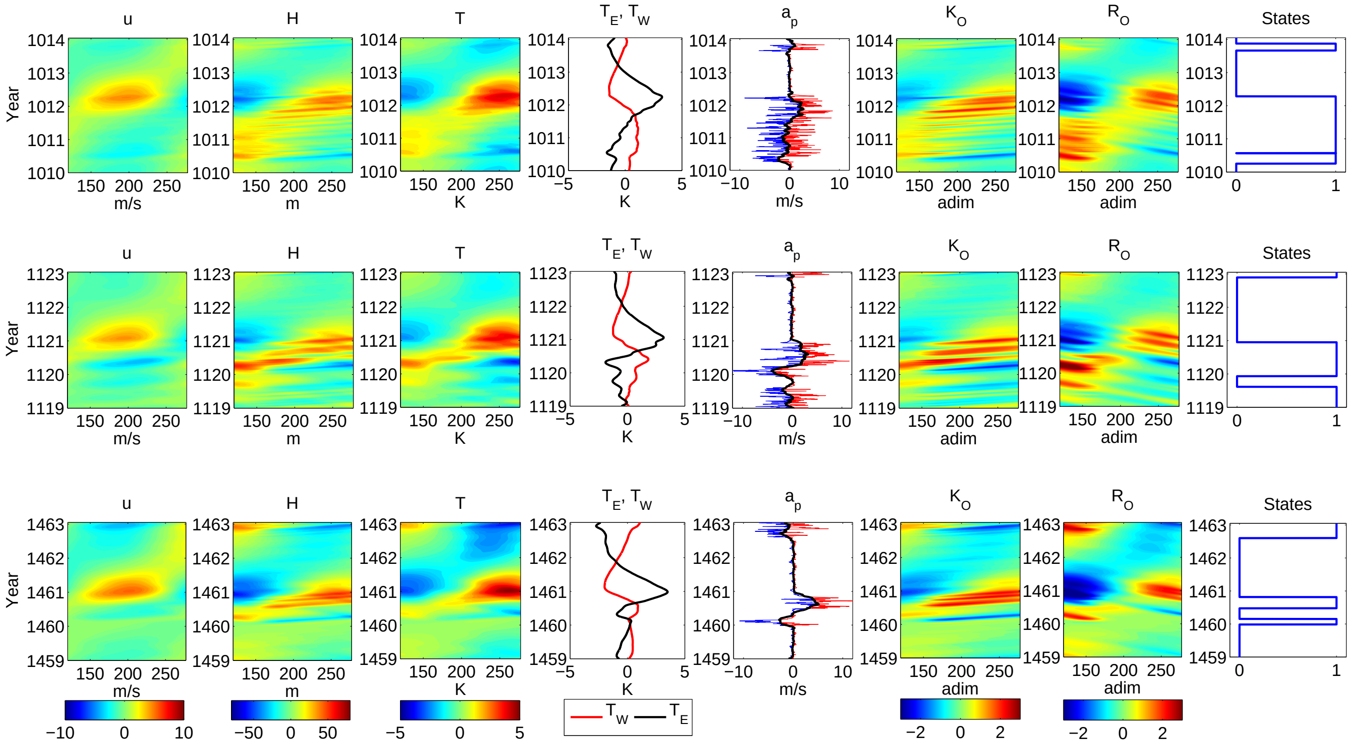

Fig. S4 Additional examples of super El Niño events in the model, as in Fig. 2 of the main article.

burst characteristics:

$$\text{if } s = \begin{cases} 0 \text{ then } \sigma_p = 0.5, \quad d_p = 5.1, \, \hat{a}_p = 0 \qquad\quad \text{(Quiescent State)}, \\ 1 \text{ then } \sigma_p = 1.2, \quad d_p = 5.1, \, \hat{a}_p = -0.25 \text{ (Active State CP)}, \\ 2 \text{ then } \sigma_p = 3.75, \, d_p = 5.1, \, \hat{a}_p = -0.25 \text{ (Active State EP)}. \end{cases} \tag{16}$$

The quiescent state 0 models conditions in the absence of El Niño activity or during La Niña with weak wind burst activity σ_p and no mean trade winds strengthening $\hat{a}_p$. The active state 1 models conditions during periods with Central Pacific El Niño events with moderate wind burst activity and enhanced mean trade winds (e.g. as observed in the 1990s). The active state 2 models conditions during traditional Eastern Pacific El Niño events with strong wind burst activity as well as enhanced mean trade winds kept for consistency with the other active state 1. The dissipation rate d_p (around 6.7 days) is identical in each state. The probabilities of transiting from a given state i to another state $j \neq i$ or to remain in the same state i after a time interval $\Delta\tau$ read:

$$\begin{aligned} &P(s(\tau + \Delta\tau) = j \,|s(\tau) = i) = \mu_{ij} \Delta\tau + o(\Delta\tau), \\ &P(s(\tau + \Delta\tau) = i \,|s(\tau) = i) = 1 - \textstyle\sum_{i \neq j} \mu_{ij} \Delta\tau + o(\Delta\tau). \end{aligned} \tag{17}$$

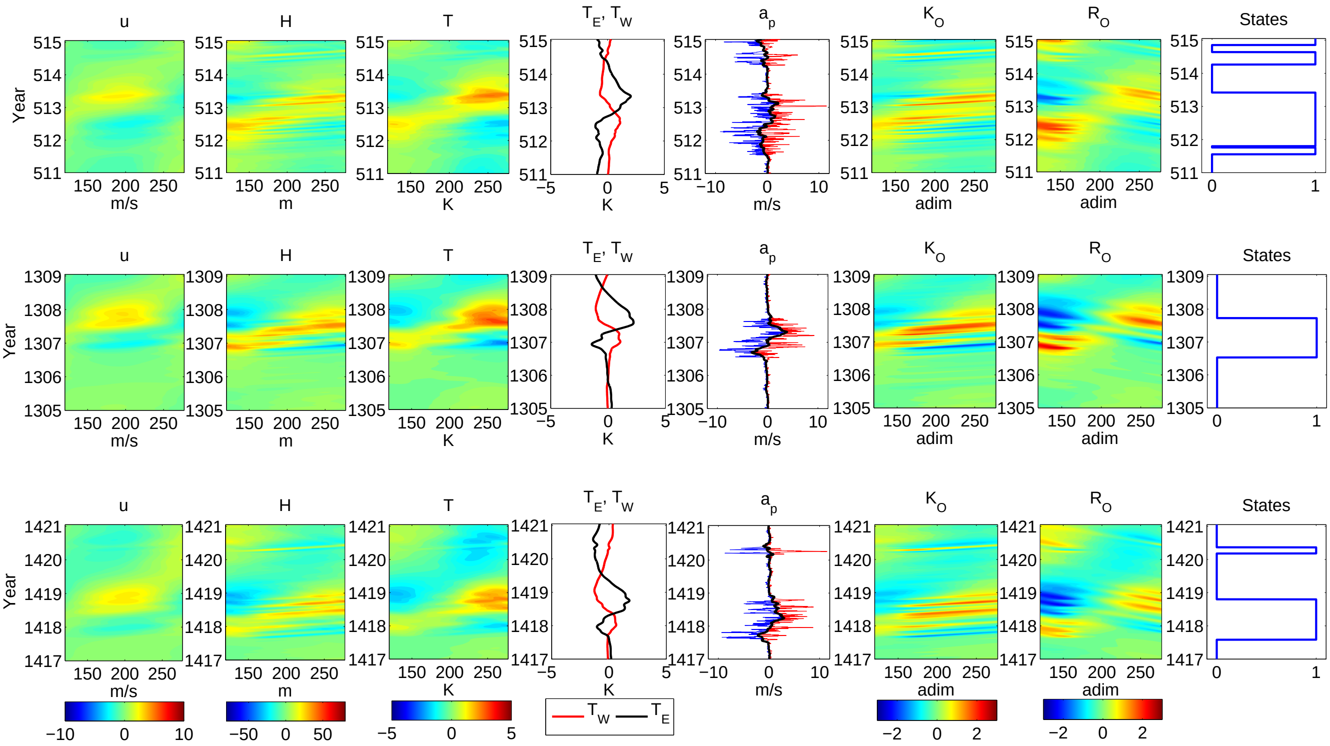

Fig. S5 Additional examples of moderate El Niño events in the model.

Importantly, the transitions rates μ_{ij} are state-dependent on the warm pool strength, i.e. on T_W the average of SST anomalies in the western half of the equatorial Pacific, according to the simple general relationship:

$$\begin{aligned} \mu_{ij} &= (1 + \tanh(2T_W))/r_{ij} \text{ if } i < j, \\ \mu_{ik} &= (1 - \tanh(2T_W))/r_{ik} \text{ if } i > k, \end{aligned} \tag{18}$$

with coefficients r_{ij}. A stronger warm pool ($T_W \geq 0$) favors the transition to higher states with increased wind burst activity, and conversely a weaker warm pool ($T_W \leq 0$) favors the transition to lower states with decreased wind burst activity.

Fig. S7(left) shows hovmollers for the complete model's solutions. The results are comparable to Fig. 2 in the main article. In particular, the complete model realistically captures central Pacific El Niño events of varying intensity and strength in addition to the super, delayed, or moderate events in the eastern Pacific. Fig. S7(right) shows qualitative model surrogates for the 2014-2016 delayed super El Niño and the 1997-1998 super El Niño in nature. The results are comparable to Fig. 3 in the main article, with in particular wind bursts first stalling the development of the delayed super Niño before an eventual sequence of strong westerly wind bursts.

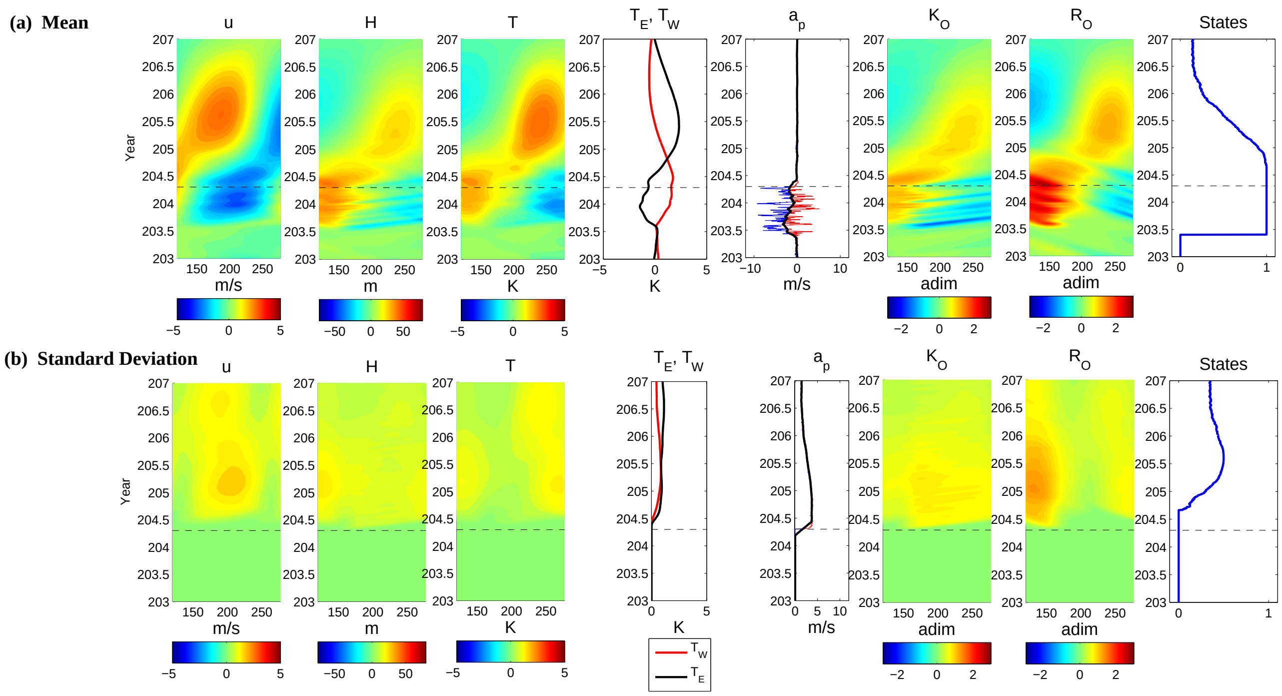

Fig. S6 Ensemble runs experiments. Hovmollers and timeseries as in Fig. 3 of the main article, but for the ensemble mean (top) and ensemble standard deviation (bottom). All ensemble members are initiated from identical initial conditions at year 204.3 (dashed line) and differ due to random wind bursts.

References

Chen N, Majda A (2016) Simple dynamical models capturing the key features of the central pacific El Nino. Proc Natl Acad Sci 113:11,732–11,737

Chen N, Majda A (2017) Simple Stochastic Dynamical Models Capturing the Statistical Diversity of El Nino Southern Oscillation. Proc Natl Acad Sci 113(42):11,732–11,737

Lawler GF (2006) Introduction to Stochastic Processes. Chapman and Hall/CRC, 192pp

Majda AJ, Harlim J (2012) Filtering Complex Turbulent Systems. Cambridge University Press

Thual S, Majda A, Chen N, Stechmann S (2016) Simple Stochastic Model for El Nino with Westerly Wind Bursts. Proc Natl Acad Sci 113(37):10,245–10,250

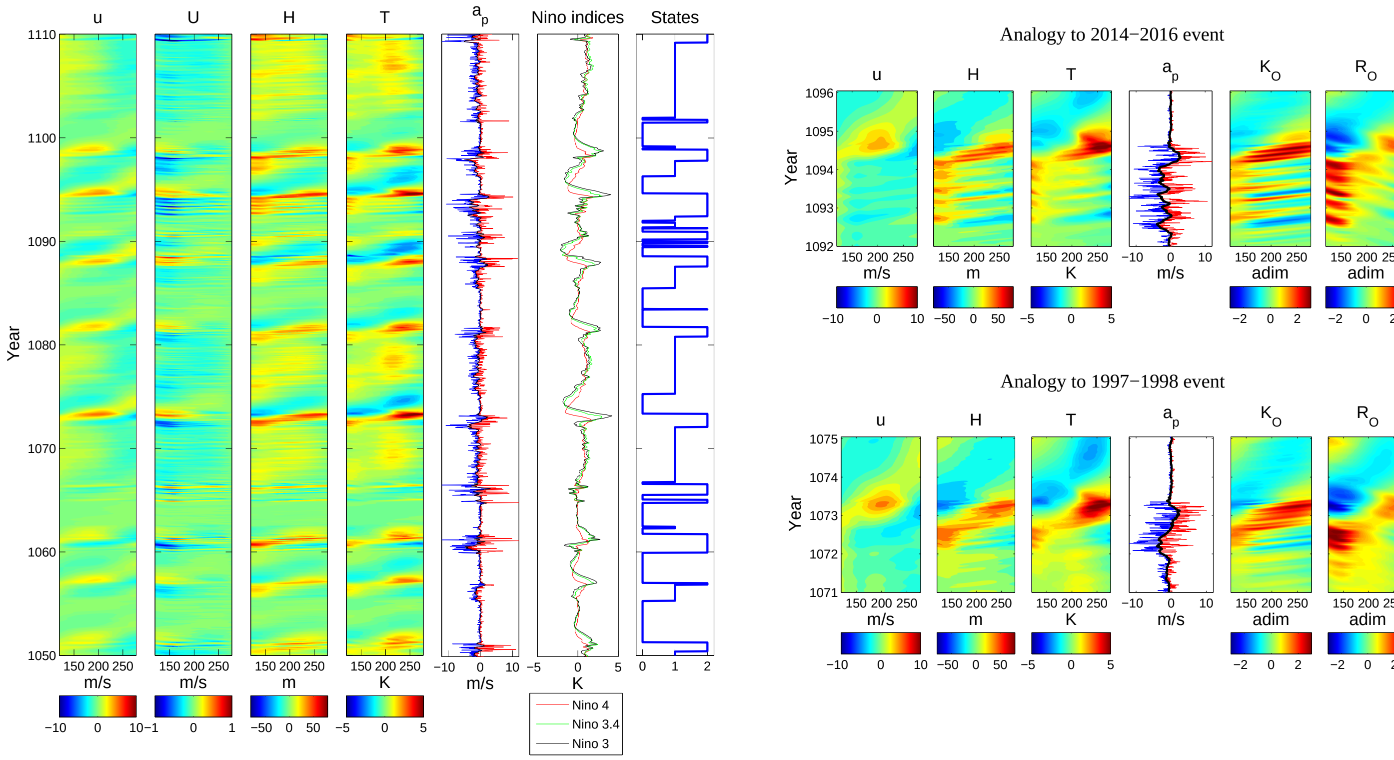

Fig. S7 Complete model version from ((Chen and Majda, 2016); 2017). (left) Hovmollers of long-term solutions. (right) Examples of model surrogates for the 2014-2016 delayed super El Niño and the 1997-1998 super El Niño in nature.